Towards Synthetic Life—Molecular Design of Complex Coacervates that Self-Divide

Authors: Monika Wenisch[1], Marius G. Braun[2], Lukas Eylert[3], Fabian Späth[1], Simone Poprawa[1], Bernhard Rieger[3], Christopher V. Synatschke[2], Job Boekhoven[1]

Affiliations:

[1] Department of Bioscience, School of Natural Sciences, Technical University of Munich, Lichtenbergstrasse 4, 85748 Garching, Germany.

[2] Synthesis of Macromolecules, Max Planck Institute for Polymer Research, Ackermannweg 10, 55128 Mainz, Germany.

[3] WACKER-Chair for Macromolecular Chemistry, Catalysis Research Center, Technical University of Munich, Lichtenbergstrasse 4, 85748 Garching, Germany.

KEYWORDS: self-division, active droplets, chemically fueled complex coacervates, synthetic life, de novo life

ABSTRACT: *Complex coacervation occurs when oppositely charged polyelectrolytes interact, leading to liquid-liquid phase separation. We coupled this phase separation to a fuel-driven reaction cycle, leading to active droplets that emerge when fuel is supplied and dissolve when the energy source is depleted. These behaviors make them an exciting protocell model and a promising step toward synthetic life. However, these active coacervate droplets cannot self-divide—critically important for Darwinian evolution and, by extension, synthetic life. This work demonstrates how to design division in active complex coacervate droplets. We found that mixtures of long and short polyanions lead to tiny speckles inside the active droplets. As the droplet dissolves, these speckles made of the long polyanion liberate as daughter droplets. In fueling-starvation-fueling experiments, we can rescue the offspring by adding the second batch of fuel. Finally, we showed that we can include molecules partitioning in the complex coacervates, which stay in the offspring until they eventually dissolve. We envision combining our self-division of self-sustaining droplets with replicators that aid the droplets can open the door to Darwinian evolution in synthetic cells.*

Introduction

Life has been defined as a self-sustaining chemical system that undergoes Darwinian evolution.[1–5] In addition, life is considered self-sustaining, self-contained, self-regulating, self-replicating, and self-organizing.[3,6–8] As a result of these properties, living systems can undergo Darwinian evolution, and a constant increase in fitness through trial-and-error is achieved.[9,10] To gain deeper insights into the origins and mechanisms of life, scientists have turned to designing model systems, such as synthetic cells, which mimic these essential life traits. An ideal synthetic cell contains all the traits above and can undergo open-ended Darwinian evolution.[11–15] Complex coacervate droplets and liposomes are promising synthetic cells since they form compartments and enrich different molecules, serving as nutrients, catalysts, or building blocks.[16–23]

This work focuses on the self-sustainment and division of complex coacervate-based synthetic cells.[24] Several approaches to dividing coacervate protocells have been described, frequently using external factors such as shear forces[25–27], mechanical pressure[28], or temperature.[29,30] Alternatively, it has been demonstrated that droplets can be divided by molecules produced within the coacervate droplet, such as proteins that form bundles that deform the coacervate phase until it is split into two droplets.[31–35] These systems use static coacervates, meaning they are close to equilibrium and do not consume energy to sustain themselves.[25,29–32] We propose to use active coacervate droplets to get closer to living cells. In this context, active droplets do not exist in equilibrium but require a chemical reaction to sustain themselves.[36,37] Theory on such droplets has predicted that active coacervate droplets can undergo division due to shape deformation despite the surface tension.[38] However, the number of examples of self-division in active coacervates is limited.

We recently found an example of active coacervate-based droplets that can self-divide.[39] These active complex coacervate droplets comprise the homo-polymeric, polydisperse RNA (polyuridylic acid, poly-U) as a polyanion and a peptide as a polycation. They are active droplets because a chemically fueled reaction cycle[40] regulates the peptide's affinity for the polyanion.[41,42] In response to fuel, these droplets emerge, and as they consume the fuel, they decay again.[43] Excitingly, we found that towards the end of such a fueling-starvation cycle, the droplets could self-divide by ripping apart into tiny daughter droplet fragments. Eventually, these fragments also dissolved.[39] As the mechanism of the division of these droplets was not understood, we could not control it. Moreover, poly-U is a critical component for the division, and as it is derived from a biological source, it suffers from batch-to-batch variations, making the self-division unpredictable, further complicating the understanding of the division.

In this work, we unveiled the underlying mechanism of the self-division of active coacervate droplets, which is related to the maturation of droplets, leading to small, glassy domains within the original droplet. Balancing the maturation rate with the lifetime of the droplets leads to tiny speckles that dissolve roughly a minute later than the original droplets. We can tune the number of offspring each droplet produces and for how long they survive. We show that additional molecules are passed from the original droplet to the

offspring. Finally, the daughters can be rescued and become the next generation when additional fuel is supplied after division. We envision the self-division mechanism as a critical development toward synthetic life. For example, when the droplets are combined with self-replicating molecules, they are passed on to the next generation through our new self-division mechanism.

Results and discussion

System design. The self-dividing, active droplets are based on complex coacervation regulated by a fuel-driven chemical reaction cycle. We used the peptide acetyl-FRGRGD-OH as polycation (peptide) in which F means phenylalanine, R means arginine, G means glycine, and D means aspartic acid.

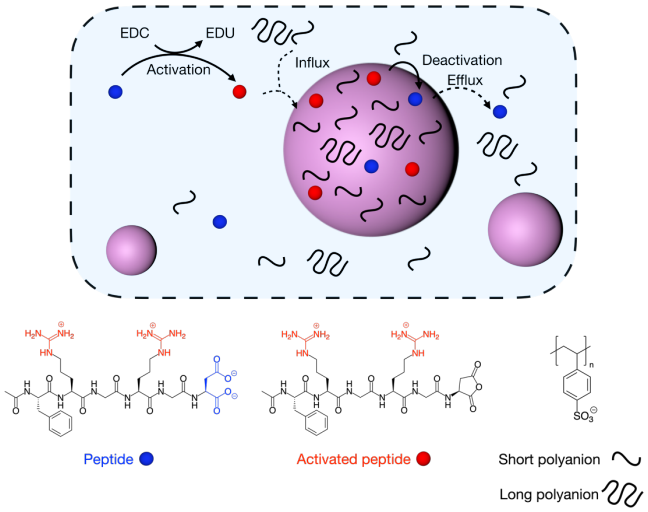

Scheme 1: Active complex coacervation coupled to a chemical reaction. A schematic representation of the chemical reaction cycle coupled to the formation of complex coacervate-based droplets. The chemical reaction cycle converts a peptide (blue) to an activated peptide (red) at the expense of the chemical fuel EDC. The activated peptide can interact with PSS to form liquid-liquid phase-separated complex coacervates. When deactivation outcompetes activation, droplets lose material until they dissolve.

Upon adding 1-ethyl-3-(3-dimethylaminopropyl) carbodiimide (EDC, fuel), the C-terminal aspartic acid reacts to its corresponding cyclic anhydride state—the peptide activation. The fuel is converted into its corresponding urea form (EDU, waste) in the activation. The cyclic anhydride of the activated peptide spontaneously hydrolyzes to yield the original peptide—the deactivation. The peptide is zwitterionic with a net charge of 0, whereas the activated peptide has an overall charge of +2. The cationization of the peptide enables it to form complex coacervates with polyanions through electrostatic interactions (Scheme 1).[44] This work explores polystyrene sulfonate (PSS) of different lengths as polyanion. The transient, activated peptide is produced as long as fuel is present and the complex coacervate droplets can be sustained. However, the droplets dissolve as soon as the peptide deactivation outcompetes activation. Coupling a fuel-driven reaction cycle with droplet material formation implies that droplets emerge in response to chemical fuel. Thus, in fueling-starvation experiments, a batch of fuel is added, and the droplets have a finite lifetime.

Mechanism of the self-division. In previous work, when homopolymeric poly-U was used as a polyanion, we found droplet self-division towards the end of their lifetime. In the last minutes of their lifetime, a large droplet would fragment into tens of smaller droplet fragments.[39] We hypothesize that the division results from the polydispersity of the polyanion. Specifically, we suspect that during the lifetime of the droplet, the long polyanion separates from the shorter polyanion and forms solid domains, a process referred to as maturation (Fig. 1A). As the droplet dissolves, the solid domains are expelled and survive longer than the main droplet.

To verify the maturing droplet mechanism and test its generalizability, we ordered analytical standards of PSS of 4.3, 261, 453, 622, and 976 kDa molecular weight corresponding to a range in the degree of polymerization of 21 up to close to 5000 (Supporting Table 1). We refer to the 4.3 kDa PSS as the "short" PSS. All others are referred to as "long" PSS. Noteworthy, all these polymers had a polydispersity index below 1.2. We used 12.3 mM peptide and combined it with 20 mM PSS (as expressed in monomer concentration) in 200 mM MES buffered water at pH 5.3. When we supplied these solutions with 75 mM EDC as fuel, the samples became measurably turbid with all PSS independent of length (Fig. S1). The turbidity decayed again with time, indicating the formation of transient assemblies that scatter light. Importantly, the samples containing long PSS regained their original transparency much later than those with short PSS, *e.g.*, after 12 minutes for short PSS and after 19 minutes for 453 kDa PSS. Moreover, confocal microscopy revealed round, micron-sized droplets for short PSS. In contrast, for all the long PSS lengths we used, we observed rugged, non-spherical agglomerates of microns in size that dissolved much later than their short PSS counterparts (Fig. S2). In conclusion, the long PSS forms more solid-like coacervates that dissolve slower than the short PSS in response to fuel, which aligns with our hypothesis of droplet division—when combined, long polyanions form solid-like coacervate-based assemblies that dissolve slower than the droplets formed by the short polyanion.

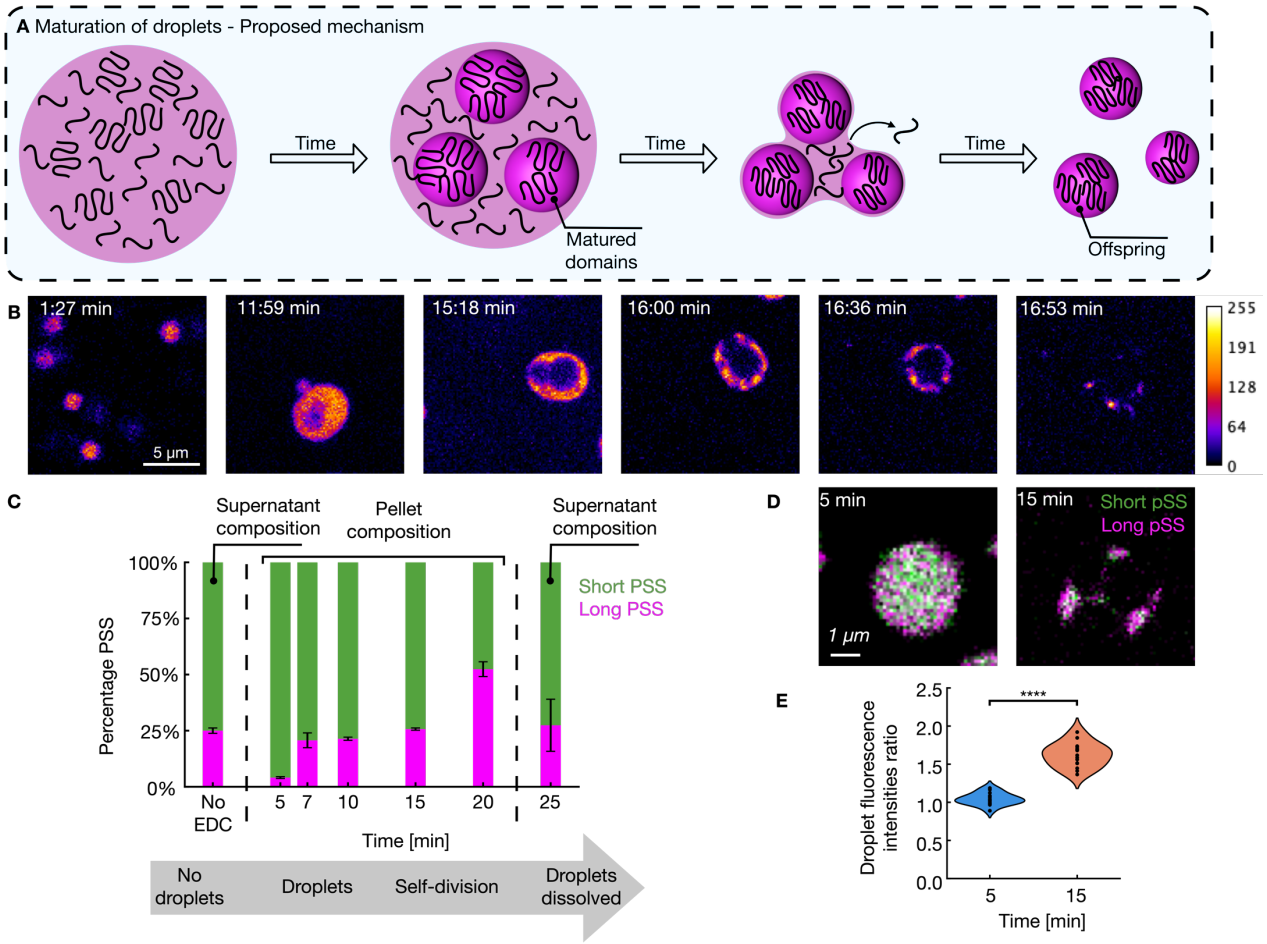

Figure 1. Droplet division with PSS with a bimodal length distribution. A) Scheme of the hypothesized mechanism of the division. Initially, the long and the short PSS are mixed inside the coacervate. Over time, the long PSS forms speckles inside the droplet. During the dissolution, the short PSS leaves the droplet first, and the speckles escape as offspring. **B**) Confocal micrographs of the reaction cycle with 12.3 mM peptide, 20 mM mixed PSS (75% 4.3 kDa PSS and 25% 622 kDa PSS, 200 mM MES buffer at pH = 5.3) and 75 mM EDC. The matured domains are observed as speckles towards the cycle end, eventually escaping as offspring. **C**) The short and long PSS percentage at different time points during the reaction cycle measured by GPC on spun down, static droplets. For the static droplets parts of the peptide were replaced by a model peptide. To determine the ratio of peptide and model peptide was determined by using a kinetic model. **D**) Merged confocal micrographs using the same conditions as in B) with labeled PSS (Cy3-PSS 10.8 kDa (green) and Cy5-PSS 404 kDa PSS (magenta), merged color: white) after 5 and 15 minutes in the reaction cycle. **E**) Droplet fluorescence ratio from the micrographs in D) (N = 15) ****P < 0.0001.

Excitingly, when we used mixtures of short and long PSS as the polyanion, we observed that the droplets self-divided through a similar fragmentation mechanism observed for poly-U. Specifically, we prepared droplets like the ones above but now used 25% long PSS (622 kDa) and 75% short PSS and imaged their behavior by confocal microscopy. The droplets consisting of PSS mixtures had a lifetime measured by turbidimetry of 17 minutes, *i.e.*, between short and long PSS lifetimes. Moreover, the long-to-short PSS ratio could tune the lifetime (Fig. S3A). Confocal microscopy revealed that the mixed PSS droplets were spherical and could fuse, from which we conclude they were liquid (Fig. S3B). When we fueled the solution with 75 mM EDC, we observed the droplets' emergence and fusion in the first minutes of the reaction cycle. Toward the end of the reaction cycle, vacuoles inside the droplets appeared (Fig. 1B), which we previously attributed to a mechanism in which the efflux of deactivated droplet material outcompetes the influx of activated droplet material.[45] Around the same time, we observed the first speckles inside the remaining droplet shell. These speckles were liberated and are independent droplet fragments that survived for tens of seconds until they finally dissolved (Fig. 1B). Using only short PSS under the same conditions showed no vacuole, speckle formation, or division (Fig. S4). These findings support our hypothesis that the long PSS forms solid-like domains inside the liquid coacervate phase that dissolve slightly later than the rest of the droplet.

We analyzed the PSS composition of the droplet to validate the mechanism by spinning down the droplet phase and analyzing it using gel permeation chromatography (GPC). Because of the dynamic nature of the active droplets and the long centrifugation times required, we used static droplets as a model instead. We mutated the aspartic acid of the peptide with an asparagine. This model for the activated peptide has an overall charge of +2 and is structurally similar to the activated peptide but does not hydrolyze—we refer to it as the activated peptide model. We used our previously described kinetic model to predict the concentration of the activated peptide at different time points in the reaction cycle.[44]

The solution of static droplets was then prepared with a mixture of short and long PSS, the peptide, and the model for the activated peptide. GPC showed that the droplets early in the cycle mainly comprised the short PSS. As the droplets progressed in the reaction cycle and less activated peptides became available, their composition shifted towards long, such that, after 20 minutes, the droplets were made of 80% long PSS (Fig. 2C). In other words, a mixture that resembles the young droplets seem to favor short PSS whereas older droplet comprises mostly long PSS.

We verified the droplet composition also changes in dynamically evolving droplets by confocal microscopy using short (10.8 kDa) Cy3-labeled PSS and long Cy5-labeled PSS (404 kDa). Indeed, the merged confocal micrographs (green short PSS and magenta long PSS) show a transition of white droplets, meaning both PSS lengths are mixed in the coacervate phase in the beginning to nearly completely magenta speckles and at the end of the reaction cycle and magenta offspring droplets (Fig. 2D, intensity line plot Fig. S5). In addition, we measured the ratio between the intensities of short and long PSS of coacervate droplets 5 min and 15 min after adding fuel. Five minutes after the fuel addition, the ratio of the fluorescence intensities of the short and long PSS was roughly 1.0. After 15 minutes, the ratio shifted to 1.6, meaning the long PSS was enriched in the coacervate droplet towards the end of the reaction cycle (Fig. 1E). The confocal microscope findings support the hypothesized mechanism of the division that short PSS is expelled first, while more solid domains comprising the long PSS remain.

Taken together, the active droplets consist of a mixture of long and short PSS. During the droplets' short lifetimes, the long PSS forms mature domains as speckles within the droplets. As the fuel depletes, the activated peptide population decreases, preferentially expelling the short PSS. The speckles are expelled from the mother droplet in its final minutes. The offspring speckles move independently in the reaction solution until they finally dissolve.

With our mechanistic insights, we tested which parameters affect the droplet division. Given our interest in using these droplets for the *de novo* synthesis of life, we focussed on tuning the offspring's lifetime and number. To quantify the division, we used continuously imaged microfluidic reactors because, in such reactors, only one large droplet is produced, facilitating the quantification of the self-division process. Using the abovementioned conditions, microreactors were produced by combining peptide, PSS, and fuel in a buffered aqueous solution. Immediately after mixing, 5 µL of this aqueous solution was transferred to 50 µL of fluorinated oil and mixed gently. The resulting emulsion comprised millions of polydisperse water droplets ranging from tens to hundreds of microns in diameter—the microreactors. Within these microreactors, we observed the formation of coacervate-based droplets. We imaged the entire reactor in X, Y, and Z with time intervals of roughly 10 seconds until all the droplets had dissolved (Fig. 2A-B).

Early in the cycle, we observed multiple coacervate droplets that rapidly grew and sank to the bottom of the reactor, where they fused until only one droplet remained. We chose to image with a diameter of roughly 35 µm such that the volume of the final droplet was similar from reactor to reactor at roughly 460 μm^3 (Fig. S6). In line with the bulk microscopy data, after roughly 17 minutes, the division process started and produced tens of offspring droplets (Fig. 2B, supporting movie 1). To quantify the division process, we projected all Z-planes of one microreactor to one plane (Fig. 2C). In the Z-plane projection, we observed the formation of vacuoles, the formation of speckles, and, a few seconds later, the liberation of the speckles as droplet fragments from which we conclude the droplets in the confined space of a microreactor behave similarly to those in bulk. We wrote a Python script that counts the droplets in each frame of the confocal videos (See SI), which revealed the number of droplets rapidly decreased to one because of the fusion. After 17 minutes, the number of droplets increased from one (the "mother") to an average of 12 (the "offspring") before rapidly decreasing when all offspring dissolved.

We analyzed the influence of the mother droplet size, the fraction of long PSS, and its length on the division mechanism. First, we varied the size of the mother droplet by analyzing different microreactor sizes. An increased microreactor volume increases the droplet material and, thus, a larger coacervate droplet after fusion (Fig. S6). We found that droplets smaller than roughly 145 μm^3, *i.e.*, those with a 3.3. µm radius showed no division. From there on, the number of offspring fragments increased with the size of the initial coacervate droplet until it leveled off at, on average, 23 offspring (Fig. 2E). Increasing the coacervate droplet size also increased the variability in the offspring number. We hypothesize that critical droplet size is needed to accumulate sufficient long PSS to produce at least two speckles. Besides, larger droplets lead to more speckles.

Next, we analyzed the influence of the fuel concentration. Low fuel amounts lead to short-lived droplets, offering less time for the long PSS to mature and form speckles (Fig. S7). Indeed, we found that the coacervates fueled with 25 mM EDC did not show division. Fueling with 50 and 75 mM EDC leads to, on average, eight offspring droplets. Surprisingly, using 100 mM EDC or more decreases the offspring to roughly three (Fig. 2F). We assume that with the increasing lifetime of the droplets, the chance that speckles combine increases, leading to fewer offspring. The amount of EDC we used did not influence the offspring's lifetime (Fig. S8).

Next, we kept the total PSS concentration constant at 20 mM as expressed as monomers but varied the fraction of long PSS from 0% to 65%. Increasing the fraction of long PSS leads to the formation of increasingly more viscous droplets, as measured by FRAP experiments (Fig. S9). We observed that droplets without long PSS dissolve homogeneously without producing any offspring (Fig. 2G). In contrast, droplets with as little as 10% PSS displayed a few speckles and consistently produced droplet fragments, albeit only a few. With an increasing fraction of PSS, the number of offspring increased. However, when we tested 40% long PSS or more, the fusion of the droplets was so slow that the initial droplet was rugged and inhomogeneous. At 65% of long PSS, it became evident that the large droplet was merely a conglomerate of the droplets but so viscous that they did not fuse. While the dissolution led to droplet fragments, it was clear that the fragments were simply the remnants of the original, unfused droplets. Given that the original droplets were never homogeneous, we argue that this process is hard to define as division.

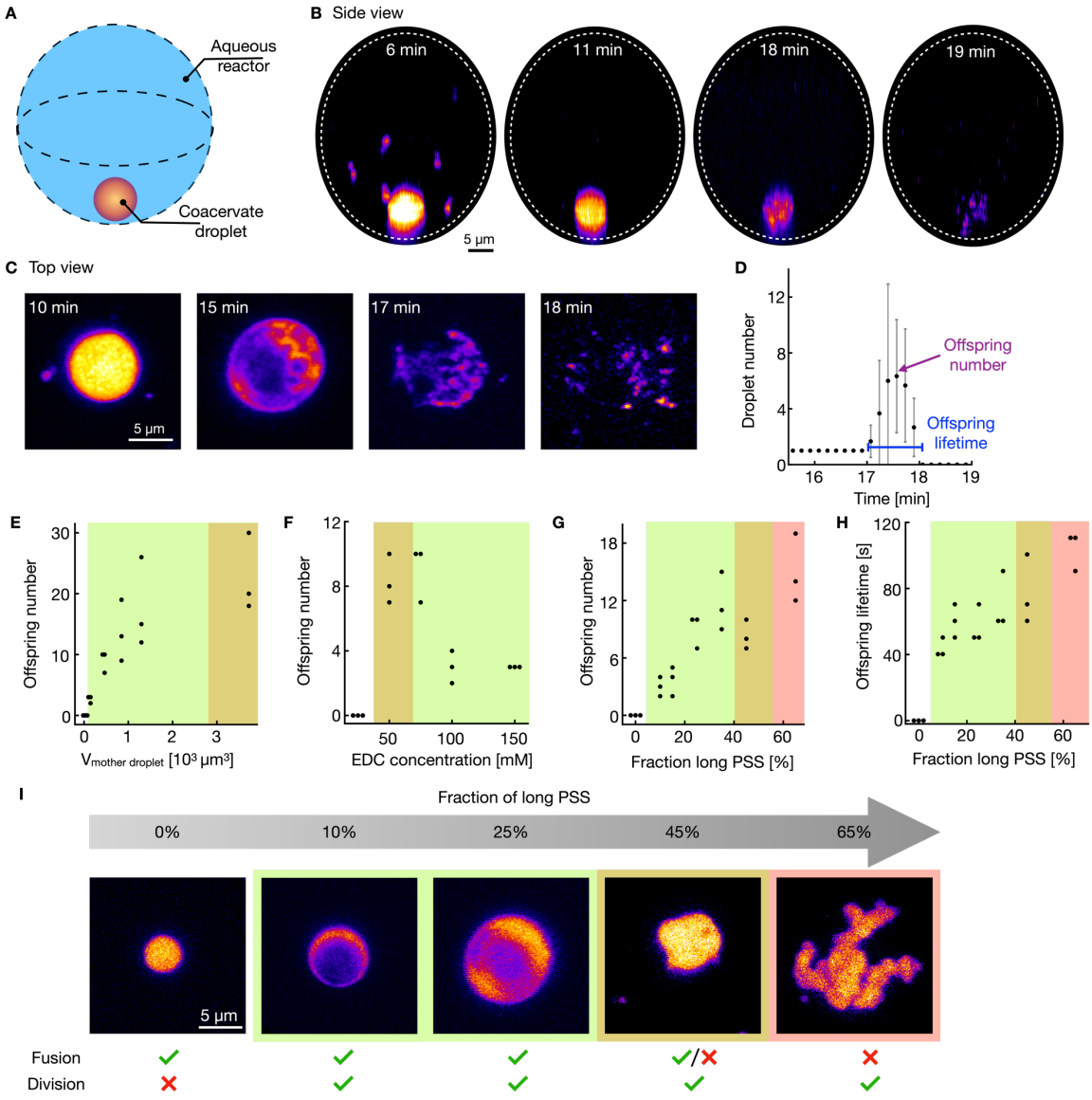

Figure 2: Quantification and controlling of the division. A) Schematic representation of microreactors with one droplet. **B**) Confocal micrographs of the side view of a microreactor using 12.3 mM peptide, 20 mM PSS (75% 4.3 kDa PSS and 25% long PSS, expressed in monomer units), 200 mM MES buffer at pH = 5.3, and 75 mM EDC. **C**) Confocal micrographs of the top view of the microreactor (z-projection) using the same conditions as in B. **D**) The droplet number over time in a microreactor, the error bars represent the standard deviation (N = 3). **E-I**) Green background indicating fast fusion, orange slow fusion and red no fusion to a spherical droplet. **E**) Offspring number as a function of the coacervate volume of the "mother" droplet under the same conditions as in B. **F**) Influence of the EDC concentration on the offspring number over EDC concentration using 12.3 mM peptide, 20 mM PSS (75% 4.3 kDa PSS and 25% long PSS, expressed in monomer units), 200 mM MES buffer at pH = 5.3. **G**) Offspring number as a function of the fraction of long PSS using 12.3 mM peptide, 20 mM PSS (expressed in monomer units), 200 mM MES buffer at pH = 5.3, and 75 mM EDC. **H**) Offspring lifetime over long PSS fraction using the same conditions as in G. **I**) Confocal micrographs of the same samples as in G and H.

We also analyzed the offspring's lifetime, which increased with increasing ratio of long PSS from an average of 40 seconds to 70 seconds from 10% to 35%, respectively (Fig. 2H). Finally, we tested the length of the long PSS on the droplet division behavior and found that a long PSS of 261 kDa at 25% did not produce any droplet fragments. Lengths beyond 261 kDa consistently produced offspring with nearly identical lifetimes (Fig. S10). We conclude that the division mechanism is a concerted effort between the short and long PSS—the short is required to produce liquid droplets that enable the long PSS to mature in the next generation of droplets. Too much short PSS hardly produces offspring. Too much long PSS prevents the fusion into the necessary droplet for maturation.

In our vision of *de novo* synthesis of life, self-division is critical. Nevertheless, equally important is that the offspring droplets can become the next generation of droplets upon refueling (Fig. 3A). In this context, a speckle liberated in the form of an offspring droplet should serve as a nucleus for the growth when fuel is available again while suppressing the nucleation of new droplets. We refer to such a droplet as a second-generation droplet. Thus, experimentally, the exact timing of the refueling is critical. Too early in the cycle leads to a regrowth of all mother droplets, and too late results in the complete dissolution of all droplets and a reset of the system (see Fig. S11).

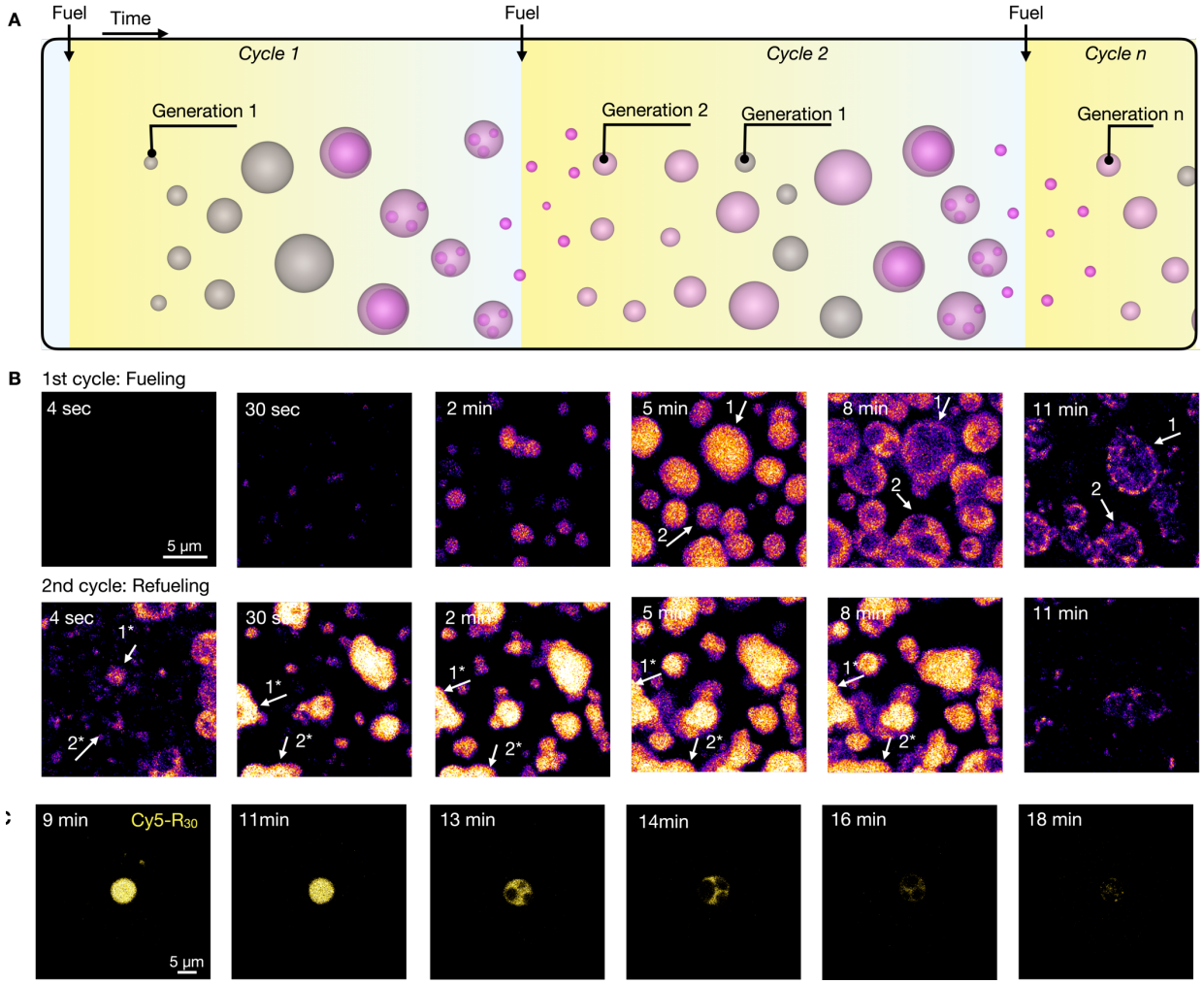

Figure 3: Rescuing the offspring droplets by adding another batch of fuel and generating a second generation. A) A scheme of the coacervation formation coupled to the reaction cycle with self-division at the end and rescuing the offspring droplets to form a second generation of coacervates. **B**) Confocal micrographs of refueling experiments using 12.3 mM peptide, 20 mM PSS (75% 4.3 kDa PSS and 25% long PSS, expressed in monomer units), 200 mM MES buffer at pH = 5.3, and 50 mM EDC. The offspring droplets were rescued by adding another 50 mM EDC after 11 min. **C**) Confocal micrographs of a sample with a positively charged peptide, a model replicator, using 12.3 mM peptide, 20 mM PSS (75% 4.3 kDa PSS and 25% long PSS, expressed in monomer units), 200 mM MES buffer at pH = 5.3, 500 nM Cy5-R30, and 75 mM EDC.

We tested the refueling experiments using 12.3 mM peptide, 20 mM PSS with 75% short PSS, and 25% long PSS fueled with 50 mM EDC. The first coacervate droplets could be observed 30 seconds after the first fuel addition (Fig. 3B). The droplets grew and fused for several minutes. After roughly eleven minutes, the vacuolization started, followed by the speckle formation and the liberation into offspring. After 11 minutes, we added a second batch of 50 mM fuel. Because of the flow induced by adding a second batch of fuel, it could be hard to track the offspring droplets. We tracked a few droplets and found that their size increased quickly after adding fuel, e.g., from 1 to 1* in Fig. 3B, and more examples in Fig. S12. 30 seconds after the second fuel addition, we observed a bigger and smaller population of droplets in the sample. We assume that the bigger ones originated from the offspring droplets and thus are second-generation droplets. The smaller droplets were freshly nucleated, the new first generation. We found the resulting second-generation droplet to be more viscous in the first few minutes than the first-generation. The fusion with other droplets is slower, resulting in non-spherical droplets. Over time, the second-generation droplet takes up more short PSS, resulting in a less viscous droplet that fuses more easily. Towards the end, the vacuole formation, followed by the speckles formation, is observed. Finally, the coacervate droplets' division occurs (Fig. 3B, supporting movie 2). We conclude that we can rescue the offspring by adding a second batch of fuel. In addition, the division mechanism is not affected by the second fuel addition nor by the different morphology of the second-generation droplets due to the initially higher long PSS content.

Rescuing the offspring droplets with another batch of fuel is exciting, as it means that the identity of the droplets is not wiped out with every refueling experiment. Ideally, information-containing molecules (like a synthetic genotype) are passed on from the mother to the offspring. As our system does not contain any such genotype, we tested whether such experiments are positive with labeled, positively charged peptide (Cy5-R_{30}) as a model. The R_{30} is homogenously distributed in the coacervate during the reaction cycle. Towards the end of the cycle, the R_{30} remains in the offspring droplets until they eventually dissolve (Fig. 3C). In other words,

positively charged molecules like R_{30} are passed from the mother droplet to the offspring.

Discussion

To synthesize *de novo* life, we require compartments that can undergo Darwinian evolution. Darwinian evolution is impossible without an analog to a genotype, *i.e.*, information-containing molecules that affect the traits of the compartments and are passed on between generations. The genotype and the compartments must be replicated to ensure that daughter compartments receive these information-containing molecules without dilution over generations. Mutations in the replication process are also needed to increase the genotype space. Finally, selection pressures can select fitter mutants over less fit ones.

Our work addresses one step in this vision towards *de novo* life—the division of the non-equilibrium compartments into daughter compartments. The division we showed is environment-dependent—when the environment is almost depleted of fuel, the mother droplet releases its offspring. It is questionable how "self" the self-division is in this scenario, but we argue that self-division of life as we know it is also strongly environment dependent—cells only divide when fed with sufficient nutrients. Conceptually, the division we demonstrated is closer to fungal sporulation—a mechanism by which fungi spread offspring during harsh conditions (in our case, starvation) to respawn when conditions are more favorable (in our case, when fuel is abundant).

The resulting offspring in our work has no genotype, *i.e.*, information containing molecules passed on from the mother compartment. We envision that such a genotype can come from a self-replicating molecule that, during the short lifetime of the mother, is replicated at least as often as the number of offspring droplets produced. Given the roughly 12 droplets produced per mother droplet, that would imply one molecule of "genotype" needs to undergo four replication cycles during the roughly 10-minute lifetime of the mother to ensure that, statistically speaking, each daughter could receive one molecule of "genotype". Thus, replication should be fast, on the order of a few minutes per replication cycle. These replicating molecules should affect the behavior of the compartments, a minimal analog of genotype-phenotype mapping. Our work already offers a glimpse of how that could be possible—long polyanions induce the ability to produce offspring. Put differently, if a replicating molecule produces long polyanions (or is a long polyanion itself), it can change the droplet phenotype by enabling its division. Another mechanism could involve the replicator extending the lifetime of the compartment so that it survives until the next fueling round.

Conclusion

We studied the mechanism of the fragmentation of active droplets and tested different parameters to tune the fragmentation. We verified that the long PSS remains inside slightly longer than the coacervate droplets than the short PSS, providing the long PSS enough time to mature inside the coacervate droplet to form denser domains, which are then liberated. Adding a second batch of chemical fuel at the right time can rescue the offspring. Their growth is faster than new nucleated droplets, giving them an advantage. Our findings enable a synthetic, self-sustaining protocell to undergo growth, division, and replication by introducing a set of self-replicating molecules. The replicator should be designed so that the fragments that contain a replicator survive longer than the ones without. The longer-lived fragments can survive longer until the next batch of fuel is needed. Such coupling between a primitive genotype and phenotype could lead to Darwinian evolution in a synthetic system.

ASSOCIATED CONTENT

Supporting Information

Materials and Methods description and additional data (Synthetic protocols and analysis; Sample preparation; HPLC analysis; kinetic model; Turbidity Measurements; Confocal Fluorescence Microscopy; FRAP procedures) (PDF)

Movie of the side view of a water reactor with complex coacervates that divide in a confocal microscope (avi)

Confocal microscope movie of the experiment of fueling and refueling the complex coacervates (mp4)

AUTHOR INFORMATION

Corresponding Author

Job Boekhoven – Department of Chemistry and Institute for Advanced Study, Technical University of Munich, 85748 Garching, Germany; orcid.org/0000-0002-9126-2430; Email: job.boekhoven@tum.de

Authors

Monika Wenisch – Department of Chemistry, Technical University of Munich, 85748 Garching, Germany

Marius Braun – Max Planck Institute for Polymer Research, 55128 Mainz, Germany

Fabian Späth – Department of Chemistry, Technical University of Munich, 85748 Garching, Germany

Simone Poprawa – Department of Chemistry, Technical University of Munich, 85748 Garching, Germany

Lukas Eylert – WACKER-Chair of Macromolecular Chemistry, Catalysis Research Center, Technical University of Munich, 85748 Garching, Germany

Bernhard Rieger – WACKER-Chair of Macromolecular Chemistry, Catalysis Research Center, Technical University of Munich, 85748 Garching, Germany; orcid.org/0000-0002-0023-884X

Christopher V. Synatschke – Max Planck Institute for Polymer Research, 55128 Mainz, Germany

Author Contributions

The manuscript was written through the contributions of all authors. All authors have approved the final version of the manuscript.

Notes

The authors declare no competing financial interest.

ACKNOWLEDGMENT

The BoekhovenLab is grateful for support by the TUM Innovation Network - RISE funded through the Excellence Strategy and the European Research Council (ERC starting grant 852187). This research was conducted within the Max Planck School Matter to Life supported by the German Federal Ministry of Education and Research (BMBF) in collaboration with the Max Planck Society. Funded by the Deutsche Forschungsgemeinschaft (DFG, German Research Foundation) under Germany's Excellence Strategy - EXC-2094 – 390783311. We thank Christine Rosenauer (MPI Mainz) for her assistance with the GPC analysis.

ABBREVIATIONS

EDC, 1-ethyl-3-(3-dimethylaminopropyl); PSS, polystyrene sulfonate; EDU, 1-[3-(dimethylamino)propyl]-3-ethylurea; poly-U, polyuridylic acid.

REFERENCES

(1) Galimov, E. M. Phenomenon of Life: Between Equilibrium and Non-Linearity. *Orig. Life Evol. Biosphere J. Int. Soc. Study Orig. Life* **2004**, *34* (6), 599–613. https://doi.org/10.1023/b:orig.0000043131.86328.9d.

(2) Goodson, M. L.; Knotts, T. A.; Campbell, E. L.; Snyder, C. A.; Young, B. M.; Privalsky, M. L. Specific Ablation of the NCoR Corepressor δ Splice Variant Reveals Alternative RNA Splicing as a Key Regulator of Hepatic Metabolism. *PLoS ONE* **2020**, *15* (10), e0241238. https://doi.org/10.1371/journal.pone.0241238.

(3) Macklem, P. T.; Seely, A. Towards a Definition of Life. *Perspect. Biol. Med.* **2010**, *53* (3), 330–340. https://doi.org/10.1353/pbm.0.0167.

(4) Gómez-Márquez, J. What Is Life? *Mol. Biol. Rep.* **2021**, *48* (8), 6223–6230. https://doi.org/10.1007/s11033-021-06594-5.

(5) Macklem, P. T.; Seely, A. Towards a Definition of Life. *Perspect. Biol. Med.* **2010**, *53* (3), 330–340.

(6) Bissette, A. J.; Fletcher, S. P. Mechanisms of Autocatalysis. *Angew. Chem. Int. Ed Engl.* **2013**, *52* (49), 12800–12826. https://doi.org/10.1002/anie.201303822.

(7) Lai, Y.-C.; Chen, I. A. Protocells. *Curr. Biol.* **2020**, *30* (10), R482–R485. https://doi.org/10.1016/j.cub.2020.03.038.

(8) Szathmáry, E.; Santos, M.; Fernando, C. Evolutionary Potential and Requirements for Minimal Protocells. In *Prebiotic Chemistry*; Walde, P., Ed.; Springer: Berlin, Heidelberg, 2005; pp 167–211. https://doi.org/10.1007/tcc001.

(9) Baum, D. A.; Peng, Z.; Dolson, E.; Smith, E.; Plum, A. M.; Gagrani, P. The Ecology–Evolution Continuum and the Origin of Life. *J. R. Soc. Interface* *20* (208), 20230346. https://doi.org/10.1098/rsif.2023.0346.

(10) Bowler, P. J. *The Eclipse of Darwinism: Anti-Darwinian Evolution Theories in the Decades Around 1900*; JHU Press, 1983.

(11) Solé, R. V. Evolution and Self-Assembly of Protocells. *Int. J. Biochem. Cell Biol.* **2009**, *41* (2), 274–284. https://doi.org/10.1016/j.biocel.2008.10.004.

(12) Noireaux, V.; Maeda, Y. T.; Libchaber, A. Development of an Artificial Cell, from Self-Organization to Computation and Self-Reproduction. *Proc. Natl. Acad. Sci. U. S. A.* **2011**, *108* (9), 3473–3480. https://doi.org/10.1073/pnas.1017075108.

(13) Koshland, D. E. The Seven Pillars of Life. *Science* **2002**, *295* (5563), 2215–2216. https://doi.org/10.1126/science.1068489.

(14) Otto, S. Dynamic Molecular Networks: From Synthetic Receptors to Self-Replicators. *Acc. Chem. Res.* **2012**, *45* (12), 2200–2210. https://doi.org/10.1021/ar200246j.

(15) Kriebisch, C.; Bantysh, O.; Baranda, L.; Belluati, A.; Bertosin, E.; Dai, K.; Roy, M. de; Fu, H.; Galvanetto, N.; Gibbs, J.; Gomez, S. S.; Granatelli, G.; Griffo, A.; Guix, M.; Gurdap, C. O.; Harth-Kitzerow, J.; Haugerud, I.; Häfner, G.; Jaiswal, P.; Javed, S.; Karimi, A.; Kato, S.; Kriebisch, B.; Laha, S.; Lee, P.-W.; Lipinski, W.; Matreux, T.; Michaels, T.; Poppleton, E.; Ruf, A.; Slootbeek, A.; Smokers, I.; Soria-Carrera, H.; Sorrenti, A.; Stasi, M.; Stevenson, A.; Thatte, A.; Tran, M.; Haren, M. van; Vuijk, H.; Wickham, S.; Zambrano, P.; Adamala, K.; Alim, K.; Andersen, E. S.; Bonfio, C.; Braun, D.; Frey, E.; Gerland, U.; Huck, W.; Jülicher, F.; Laohakunakorn, N.; Mahadevan, L.; Otto, S.; Saenz, J.; Schwille, P.; Göpfrich, K.; Weber, C.; Boekhoven, J. A Roadmap towards the Synthesis of Life. ChemRxiv July 10, 2024. https://doi.org/10.26434/chemrxiv-2024-tnx83.

(16) Huang, F.; Xue, H.; Fu, Y.; Ouyang, Y.; Chen, D.; Xia, F.; Willner, I. Three Compartment Liposome Fusion: Functional Protocells for Biocatalytic Cascades and Operation of Dynamic DNA Machineries. *Adv. Funct. Mater.* **2023**, *33* (37), 2302814. https://doi.org/10.1002/adfm.202302814.

(17) Monnard, P.-A.; Deamer, D. W. Nutrient Uptake by Protocells: A Liposome Model System. *Orig. Life Evol. Biosph.* **2001**, *31* (1), 147–155. https://doi.org/10.1023/A:1006769503968.

(18) McTigue, W. C. B.; Perry, S. L. Design Rules for Encapsulating Proteins into Complex Coacervates. *Soft Matter* **2019**, *15* (15), 3089–3103. https://doi.org/10.1039/C9SM00372J.

(19) Tang, Y.; Scher, H. B.; Jeoh, T. Industrially Scalable Complex Coacervation Process to Microencapsulate Food Ingredients. *Innov. Food Sci. Emerg. Technol.* **2020**, *59*, 102257. https://doi.org/10.1016/j.ifset.2019.102257.

(20) Poudyal, R. R.; Guth-Metzler, R. M.; Veenis, A. J.; Frankel, E. A.; Keating, C. D.; Bevilacqua, P. C. Template-Directed RNA Polymerization and Enhanced Ribozyme Catalysis inside Membraneless Compartments Formed by Coacervates. *Nat. Commun.* **2019**, *10* (1), 490. https://doi.org/10.1038/s41467-019-08353-4.

(21) Drobot, B.; Iglesias-Artola, J. M.; Le Vay, K.; Mayr, V.; Kar, M.; Kreysing, M.; Mutschler, H.; Tang, T.-Y. D. Compartmentalised RNA Catalysis in Membrane-Free Coacervate Protocells. *Nat. Commun.* **2018**, *9* (1), 3643. https://doi.org/10.1038/s41467-018-06072-w.

(22) Koga, S.; Williams, D. S.; Perriman, A. W.; Mann, S. Peptide-Nucleotide Microdroplets as a Step towards a Membrane-Free Protocell Model. *Nat. Chem.* **2011**, *3* (9), 720–724. https://doi.org/10.1038/nchem.1110.

(23) Martin, N.; Douliez, J.-P. Fatty Acid Vesicles and Coacervates as Model Prebiotic Protocells. *ChemSystemsChem* **2021**, *3* (6), e2100024. https://doi.org/10.1002/syst.202100024.

(24) Lin, Z.; Beneyton, T.; Baret, J.-C.; Martin, N. Coacervate Droplets for Synthetic Cells. *Small Methods* **2023**, *7* (12), 2300496. https://doi.org/10.1002/smtd.202300496.

(25) Matsuo, M.; Kurihara, K. Proliferating Coacervate Droplets as the Missing Link between Chemistry and Biology in the Origins of Life. *Nat. Commun.* **2021**, *12* (1), 5487. https://doi.org/10.1038/s41467-021-25530-6.

(26) van Swaay, D.; Tang, T.-Y. D.; Mann, S.; de Mello, A. Microfluidic Formation of Membrane-Free Aqueous Coacervate Droplets in Water. *Angew. Chem. Int. Ed.* **2015**, *54* (29), 8398–8401. https://doi.org/10.1002/anie.201502886.

(27) Cheung Shum, H.; Varnell, J.; Weitz, D. A. Microfluidic Fabrication of Water-in-Water (w/w) Jets and Emulsions. *Biomicrofluidics* **2012**, *6* (1), 012808. https://doi.org/10.1063/1.3670365.

(28) Fanalista, F.; Deshpande, S.; Lau, A.; Pawlik, G.; Dekker, C. FtsZ-Induced Shape Transformation of Coacervates. *Adv. Biosyst.* **2018**, *2* (9), 1800136. https://doi.org/10.1002/adbi.201800136.

(29) Ianeselli, A.; Tetiker, D.; Stein, J.; Kühnlein, A.; Mast, C. B.; Braun, D.; Dora Tang, T.-Y. Non-Equilibrium Conditions inside Rock Pores Drive Fission, Maintenance and Selection of Coacervate Protocells. *Nat. Chem.* **2022**, *14* (1), 32–39. https://doi.org/10.1038/s41557-021-00830-y.

(30) Lu, T.; Nakashima, K. K.; Spruijt, E. Temperature-Responsive Peptide–Nucleotide Coacervates | The Journal of Physical Chemistry B. *J. Phys. Chem. B* **2021**, *125* (12), 3080–3091. https://doi.org/10.1021/acs.jpcb.0c10839.

(31) Weirich, K. L.; Dasbiswas, K.; Witten, T. A.; Vaikuntanathan, S.; Gardel, M. L. Self-Organizing Motors Divide Active Liquid Droplets. *Proc. Natl. Acad. Sci.* **2019**, *116* (23), 11125–11130. https://doi.org/10.1073/pnas.1814854116.

(32) te Brinke, E.; Groen, J.; Herrmann, A.; Heus, H. A.; Rivas, G.; Spruijt, E.; Huck, W. T. S. Dissipative Adaptation in Driven Self-Assembly Leading to Self-Dividing Fibrils. *Nat. Nanotechnol.* **2018**, *13* (9), 849–855. https://doi.org/10.1038/s41565-018-0192-1.

(33) Schwille, P. Division in Synthetic Cells. *Emerg. Top. Life Sci.* **2019**, *3* (5), 551–558. https://doi.org/10.1042/ETLS20190023.

(34) Dreher, Y.; Jahnke, K.; Schröter, M.; Göpfrich, K. Light-Triggered Cargo Loading and Division of DNA-Containing Giant Unilamellar Lipid Vesicles. *Nano Lett.* **2021**, *21* (14), 5952–5957. https://doi.org/10.1021/acs.nanolett.1c00822.

(35) Dreher, Y.; Jahnke, K.; Bobkova, E.; Spatz, J. P.; Göpfrich, K. Division and Regrowth of Phase-Separated Giant Unilamellar Vesicles. *Angew. Chem. Int. Ed.* **2021**, *60* (19), 10661–10669. https://doi.org/10.1002/anie.202014174.

(36) Donau, C.; Boekhoven, J. The Chemistry of Chemically Fueled

Droplets. *Trends Chem.* **2023**, *5* (1), 45–60. https://doi.org/10.1016/j.trechm.2022.11.003.
(37) Nakashima, K. K.; van Haren, M. H. I.; André, A. A. M.; Robu, I.; Spruijt, E. Active Coacervate Droplets Are Protocells That Grow and Resist Ostwald Ripening. *Nat. Commun.* **2021**, *12* (1), 3819. https://doi.org/10.1038/s41467-021-24111-x.
(38) Zwicker, D.; Seyboldt, R.; Weber, C. A.; Hyman, A. A.; Jülicher, F. Growth and Division of Active Droplets Provides a Model for Protocells. *Nat. Phys.* **2017**, *13* (4), 408–413. https://doi.org/10.1038/nphys3984.
(39) Donau, C.; Späth, F.; Sosson, M.; Kriebisch, B. A. K.; Schnitter, F.; Tena-Solsona, M.; Kang, H.-S.; Salibi, E.; Sattler, M.; Mutschler, H.; Boekhoven, J. Active Coacervate Droplets as a Model for Membraneless Organelles and Protocells. *Nat. Commun.* **2020**, *11* (1), 5167. https://doi.org/10.1038/s41467-020-18815-9.
(40) Tena-Solsona, M.; Rieß, B.; Grötsch, R. K.; Löhrer, F. C.; Wanzke, C.; Käsdorf, B.; Bausch, A. R.; Müller-Buschbaum, P.; Lieleg, O.; Boekhoven, J. Non-Equilibrium Dissipative Supramolecular Materials with a Tunable Lifetime. *Nat. Commun.* **2017**, *8* (1), 15895. https://doi.org/10.1038/ncomms15895.
(41) Donau, C.; Späth, F.; Stasi, M.; Bergmann, A. M.; Boekhoven, J. Phase Transitions in Chemically Fueled, Multiphase Complex Coacervate Droplets. *Angew. Chem.* **2022**, *134* (46), e202211905. https://doi.org/10.1002/ange.202211905.
(42) Späth, F.; Maier, A. S.; Stasi, M.; Bergmann, A. M.; Halama, K.; Wenisch, M.; Rieger, B.; Boekhoven, J. The Role of Chemically Innocent Polyanions in Active, Chemically Fueled Complex Coacervate Droplets. *Angew. Chem. Int. Ed.* **2023**, *62* (41), e202309318. https://doi.org/10.1002/anie.202309318.
(43) Bergmann, A. M.; Donau, C.; Späth, F.; Jahnke, K.; Göpfrich, K.; Boekhoven, J. Evolution and Single-Droplet Analysis of Fuel-Driven Compartments by Droplet-Based Microfluidics. *Angew. Chem. Int. Ed.* **2022**, *61* (32), e202203928. https://doi.org/10.1002/anie.202203928.
(44) Späth, F.; Donau, C.; Bergmann, A. M.; Kränzlein, M.; Synatschke, C. V.; Rieger, B.; Boekhoven, J. Molecular Design of Chemically Fueled Peptide–Polyelectrolyte Coacervate-Based Assemblies. *J. Am. Chem. Soc.* **2021**, *143* (12), 4782–4789. https://doi.org/10.1021/jacs.1c01148.
(45) Bergmann, A. M.; Bauermann, J.; Bartolucci, G.; Donau, C.; Stasi, M.; Holtmannspötter, A.-L.; Jülicher, F.; Weber, C. A.; Boekhoven, J. Liquid Spherical Shells Are a Non-Equilibrium Steady State of Active Droplets. *Nat. Commun.* **2023**, *14* (1), 6552. https://doi.org/10.1038/s41467-023-42344-w.

Insert Table of Contents artwork here